

This article was downloaded by:

On: 25 January 2011

Access details: *Access Details: Free Access*

Publisher *Taylor & Francis*

Informa Ltd Registered in England and Wales Registered Number: 1072954 Registered office: Mortimer House, 37-41 Mortimer Street, London W1T 3JH, UK



Separation Science and Technology

Publication details, including instructions for authors and subscription information:

<http://www.informaworld.com/smpp/title~content=t713708471>

Optimization of Floc Characteristics for Treatment of Highly Turbid Water

Gurusamy Annadurai^a; S. S. Sung^a; D. J. Lee^a

^a Department of Chemical Engineering, National Taiwan University, Taipei, Taiwan

Online publication date: 08 July 2010

To cite this Article Annadurai, Gurusamy , Sung, S. S. and Lee, D. J.(2005) 'Optimization of Floc Characteristics for Treatment of Highly Turbid Water', *Separation Science and Technology*, 39: 1, 19 – 42

To link to this Article: DOI: 10.1081/SS-120027399

URL: <http://dx.doi.org/10.1081/SS-120027399>

PLEASE SCROLL DOWN FOR ARTICLE

Full terms and conditions of use: <http://www.informaworld.com/terms-and-conditions-of-access.pdf>

This article may be used for research, teaching and private study purposes. Any substantial or systematic reproduction, re-distribution, re-selling, loan or sub-licensing, systematic supply or distribution in any form to anyone is expressly forbidden.

The publisher does not give any warranty express or implied or make any representation that the contents will be complete or accurate or up to date. The accuracy of any instructions, formulae and drug doses should be independently verified with primary sources. The publisher shall not be liable for any loss, actions, claims, proceedings, demand or costs or damages whatsoever or howsoever caused arising directly or indirectly in connection with or arising out of the use of this material.

Optimization of Floc Characteristics for Treatment of Highly Turbid Water

Gurusamy Annadurai, S. S. Sung, and D. J. Lee*

Department of Chemical Engineering, National Taiwan University,
Taipei, Taiwan

ABSTRACT

This study addressed the size and fractal dimensions of flocs coagulated from highly turbid raw water using polyaluminum chloride (PACl) as the coagulant. Large flocs with loose interior structures are preferred for removing turbidity and humic acid from water. The response surface method, with the Box–Behnken design of experiments, was used to elucidate the effects of pH, turbidity, alkalinity of suspension, doses of PACl, and humic acid on the characteristics of the flocs. Nondimensional correlations between the floc size and the fractal dimension of the coagulated flocs were derived by regression analysis. Graphical presentation facilitates the interpretation of the data obtained from the designed experiments. The variable that most affects the floc characteristics is the PACl dose. However, the “optimal” conditions

*Correspondence: D. J. Lee, Department of Chemical Engineering, National Taiwan University, Taipei 106, Taiwan; Fax: +886-2-2362-3040; E-mail: djlee@ccms.ntu.edu.tw.

that lead to large flocs are different from those that lead to loose flocs. A compromise must be made to generate satisfactory flocs from highly turbid raw water. The conclusion drawn from bench tests is applicable to extremely highly turbid stormwater obtained during storm Nari on September 16–19, 2001.

Key Words: Floc properties; High turbidity waters; Coagulation; PACl; Humic acid.

INTRODUCTION

In the drinking water industry, coagulants, such as polyaluminum chloride (PACl), are added to the raw water to coagulate small particles into settleable flocs. The aim of the coagulation-sedimentation treatment is to remove the turbidity of the raw water. Several factors affect the effectiveness of the coagulation, including the alkalinity of the suspension, the turbidity of the raw water, the coagulant dose, the organic contents, and others.^[1,2] Humic substances are the organic compounds that mainly affect the coagulation processes, and their removal has been extensively researched because of their potential to be converted into trichloromethane (THM) in the disinfection stage.^[3]

Narkis and Rebhum^[4] stated that when both mineral particles and dissolved humic substances are present in solution, the latter controls coagulation. The optimal pH for removing humic acid is between 5 and 6, while that for removing clay is between 6.5 and 7.5.^[5,6] Precipitation and adsorption are the two dominant mechanisms by which organics are removed using hydrolyzing salts.^[7–9] Edwards and Amirtharajah^[6] presented a parallel-series reaction pathway for the interactions between alum and humic substances. Other investigators have refined the pathways.^[10,11]

Conventional coagulation and sedimentation is very effective for raw water of low to medium turbidity. Tropical storms often hit Pacific Rim countries, such as Taiwan, causing heavy rain and producing highly turbid stormwater. For example, on September 17, 2001, the tropical storm Nari hit Taiwan and yielded serious flooding. The raw water in the PingTsan Waterworks of the Taiwan Water Supply Corporation had an increased turbidity of over 1000 NTU for over a week, and of several hundreds of NTU for over a month. The total organic carbon (TOC) of raw water also increased to over 10 ppm. Presedimentation followed by conventional coagulation and flocculation using filters has been suggested to treat high turbidity water.^[12–16] Turbidity and organic substances are removed from water by physically separating sludge flocs. The presence of humic substances yields bulky flocs,



with settleability that is poor, causing high supernatant turbidity.^[17,18] This negative effect has been often attributed to the looseness of the floc structure induced by the strong interaction between humics and the mineral particles. Restated, since the resulting flocs have a loose structure, sweeping action by the flocs cannot efficiently remove fine particles from the water. Uniform mixing and adjusting the coagulant dose can improve the efficiency of solid–liquid separation by the flocs. In contrast, this study shows that the removal of turbidity and organics from flocs is favored by large flocs with loose interior structures.

This work examines the coagulation and sedimentation treatment of high turbidity raw water. The response surface method, using the Box–Behnken experimental design^[19] was used to determine correlations between turbidity and the humic acid level in coagulated supernatant. Small-angle light scattering tests were conducted to measure the fractal dimensions of sludge flocs.

EXPERIMENTAL

Materials and Test

All chemicals were obtained from Merck (Taiwan). Raw water samples were prepared by mixing prescribed amounts of UK ball clay powders in a stock solution of humic acid with 10^{-2} N NaClO₄ solution. The alkalinity was adjusted by adding NaHCO₃ salt. The pH was adjusted using HClO₄ and NaOH. The diameters of the clay powder have a monodispersed distribution with a mean diameter of around 4.1 μ m. The solid density was determined using a Micromeritics Accupyc 1330 pycnometer, as 2580 kg/m³. The stock solution of humic acid was first dissolved in a solution at pH 12. Next, the solution was filtered through a 0.45- μ m membrane, the pH of the filtrate was adjusted back to 7.

The humic–kaolin suspension was placed into a tank and the contents were stirred. The PACl solution was slowly injected into the tank and was stirred at 90 rpm for 1.5 min and then at 50 rpm for 8.5 min. The coagulated samples settled freely for 2 hr. Thereafter, the supernatant was carefully withdrawn from the sample. The turbidity of the supernatant was measured using a turbidimeter (HACH model 2100 AN). Before coagulation, at pH 7 and 500 ppm clay dosage, the turbidities of the synthetic raw water were about 200 NTU at various humic acid concentrations, indicating that the water was highly turbid. The solutions of humic acid (with neither clay nor PACl) had a turbidity of under 0.6 NTU, independently of their concentrations or the alkalinity of the suspensions. The effect of humic acid on the turbidity of



the suspension was, therefore, neglected in further discussion. The humic acid level in the supernatant at a dose of 14 ppm was 4.7 ppm after it was filtered with a 0.45- μm membrane.

The water samples were monitored using a small-angle laser light scattering sizer (Malvern Mastersizer 2000). This sizer is comprised of a 2 mW He-Ne laser ($\lambda = 632.8 \text{ nm}$) as the light source, an optic lens, and photosensitive detectors. The intensity I of the scattered light collected at angles between 0.01° and 32.1° was measured as a function of the wave vector, Q . The vector Q is defined as the difference between the incident and scattered wave vectors of the radiation beam in the medium. The magnitude of the wave vector is approximately

$$|\vec{Q}| = Q = \frac{4\pi n \sin(\theta/2)}{\lambda} \quad (1)$$

where n , θ , and λ are the refractive index of the medium (–), the scattered angle (–), and the wavelength of the radiation in a vacuum (m), respectively. If the inequality

$$\frac{1}{d_f} \ll Q \ll \frac{1}{d_p} \quad (2)$$

holds, then,

$$I(Q) \propto Q^{-D} \quad (3)$$

Restated, the log–log plot of I vs. Q , determined from the data collected in the scattering tests, is linear, with a gradient of $-D$. The parameter D is the mass fractal dimension of the aggregates.

The Malvern sizer was also used to measure aggregate sizes between 0.02 and 2000 μm . Each measurement took 20 s. The full Mie theory was used to analyze the interaction between particles and light, from which the projection area of particles could be recorded. A total of 30 measurements were made in each coagulation test and their average was reported. During size measurement, the sizer continuously and directly sampled waters from the stirred tank used for coagulation to minimize the possible deterioration of floc structures during sampling. Each experiment was duplicated under identical conditions. Data reproducibility was within 2% in most cases.

Experimental Design

The response surface method, using the Box–Behnken experimental design, yielded correlations between the size and fractal dimension of the



coagulated flocs. The response surface method involves an empirical model to evaluate the relationship between a set of controllable experimental factors and observed results. Factors considered included the pH, the concentration humic acid (ppm), the turbidity of the raw water (NTU), the PACl dose (ppm), and the alkalinity (ppm as NaHCO_3). They are represented by X_1 to X_5 , respectively.

The low, middle, and high levels of each variable were designated as -1 , 0 , and $+1$, respectively, as listed in Table 1. The range of the parameters examined applies to the highly turbid raw water, often found in Taiwan's

Table 1. Experimental design.

ID number	pH (X_1)	Humic acid (ppm) (X_2)	Turbidity (NTU) (X_3)	PACl (ppm) (X_4)	NaHCO_3 (ppm) (X_5)
1	5 (-1)	0 (-1)	100 (0)	100 (0)	100 (0)
2	9 (1)	0 (-1)	100 (0)	100 (0)	100 (0)
3	5 (-1)	28 (1)	100 (0)	100 (0)	100 (0)
4	9 (1)	28 (1)	100 (0)	100 (0)	100 (0)
5	7 (0)	14 (0)	0 (-1)	80 (-1)	100 (0)
6	7 (0)	14 (0)	200 (1)	80 (-1)	100 (0)
7	7 (0)	14 (0)	0 (-1)	120 (1)	100 (0)
8	7 (0)	14 (0)	200 (1)	120 (1)	100 (0)
9	7 (0)	0 (-1)	100 (0)	100 (0)	0 (-1)
10	7 (0)	28 (1)	100 (0)	100 (0)	0 (-1)
11	7 (0)	0 (-1)	100 (0)	100 (0)	200 (1)
12	7 (0)	28 (1)	100 (0)	100 (0)	200 (1)
13	5 (-1)	14 (0)	0 (-1)	100 (0)	100 (0)
14	9 (1)	14 (0)	0 (-1)	100 (0)	100 (0)
15	5 (-1)	14 (0)	200 (1)	100 (0)	100 (0)
16	9 (1)	14 (0)	200 (1)	100 (0)	100 (0)
17	7 (0)	14 (0)	100 (0)	80 (-1)	0 (-1)
18	7 (0)	14 (0)	100 (0)	120 (1)	0 (-1)
19	7 (0)	14 (0)	100 (0)	80 (-1)	200 (1)
20	7 (0)	14 (0)	100 (0)	120 (1)	200 (1)
21	7 (0)	0 (-1)	0 (-1)	100 (0)	100 (0)
22	7 (0)	28 (1)	0 (-1)	100 (0)	100 (0)
23	7 (0)	0 (-1)	200 (1)	100 (0)	100 (0)
24	7 (0)	28 (1)	200 (1)	100 (0)	100 (0)
25	5 (-1)	14 (0)	100 (0)	80 (-1)	100 (0)
26	9 (1)	14 (0)	100 (0)	80 (-1)	100 (0)
27	5 (-1)	14 (0)	100 (0)	120 (1)	100 (0)

(continued)



Table 1. Continued.

ID number	pH (X ₁)	Humic acid (ppm) (X ₂)	Turbidity (NTU) (X ₃)	PACl (ppm) (X ₄)	NaHCO ₃ (ppm) (X ₅)
28	9 (1)	14 (0)	100 (0)	120 (1)	100 (0)
29	7 (0)	14 (0)	0 (-1)	100 (0)	0 (-1)
30	7 (0)	14 (0)	200 (1)	100 (0)	0 (-1)
31	7 (0)	14 (0)	0 (-1)	100 (0)	200 (1)
32	7 (0)	14 (0)	200 (1)	100 (0)	200 (1)
33	5 (-1)	14 (0)	100 (0)	100 (0)	0 (-1)
34	9 (1)	14 (0)	100 (0)	100 (0)	0 (-1)
35	5 (-1)	14 (0)	100 (0)	100 (0)	200 (1)
36	9 (1)	14 (0)	100 (0)	100 (0)	200 (1)
37	7 (0)	0 (-1)	100 (0)	80 (-1)	100 (0)
38	7 (0)	28 (1)	100 (0)	80 (-1)	100 (0)
39	7 (0)	0 (-1)	100 (0)	100 (0)	100 (0)
40	7 (0)	28 (1)	100 (0)	100 (0)	100 (0)
41	7 (0)	14 (0)	100 (0)	100 (0)	100 (0)
42	7 (0)	14 (0)	100 (0)	100 (0)	100 (0)
43	7 (0)	14 (0)	100 (0)	100 (0)	100 (0)
44	7 (0)	14 (0)	100 (0)	100 (0)	100 (0)
45	7 (0)	14 (0)	100 (0)	100 (0)	100 (0)
46	7 (0)	14 (0)	100 (0)	100 (0)	100 (0)

rivers after the tropical storms. The independent variables X_i and the mathematical relationship between the response Y and these variables, can be approximated by a quadratic polynomial equation

$$Y = b_0 + \sum_{i=1}^5 b_i X_i + \sum_{i=1}^5 \sum_{j=1}^i b_{ji} X_i X_j \quad (4)$$

where Y = predicted response, b_0 = constant, b_i = linear coefficients ($i = 1-5$), b_{ii} = quadratic coefficients, and b_{ji} = cross product coefficients ($i \neq j$). Y represents either the floc size (d_f) or the fractal dimension (D) of sludge flocs. In either case, a total of 41 experiments were needed to estimate the coefficients in the model by multiple linear regression analysis. (Samples 41 to 47 in Table 1 corresponded to identical experimental conditions, which were listed to facilitate data analysis.) The above equation was solved using the software Design Expert (Stat-Ease Inc., Statistics Made-Easy, Minneapolis, MN, version 5.0.7.1999) to estimate the response of the independent variables.



RESULTS AND DISCUSSION

Experimental Results

Figures 1 and 2 show the size distributions and the scattered light plots for sludge samples 1 to 41, respectively. The mean floc size (d_f) and the fractal dimension (D) of the sludge flocs could be estimated from these curves. Most curves in Fig. 1 are of a monodispersed distribution. Therefore, the mean floc diameter alone could well represent the distribution of sizes of the flocs. Meanwhile, as Fig. 2 shows, the patterns for each $\log I$ vs. $\log Q$ curve are rather complex, indicating a "two-stage" regime. For instance, for the curve identified as 34, the two-step character at $-4 < \log Q < -2$ indicates

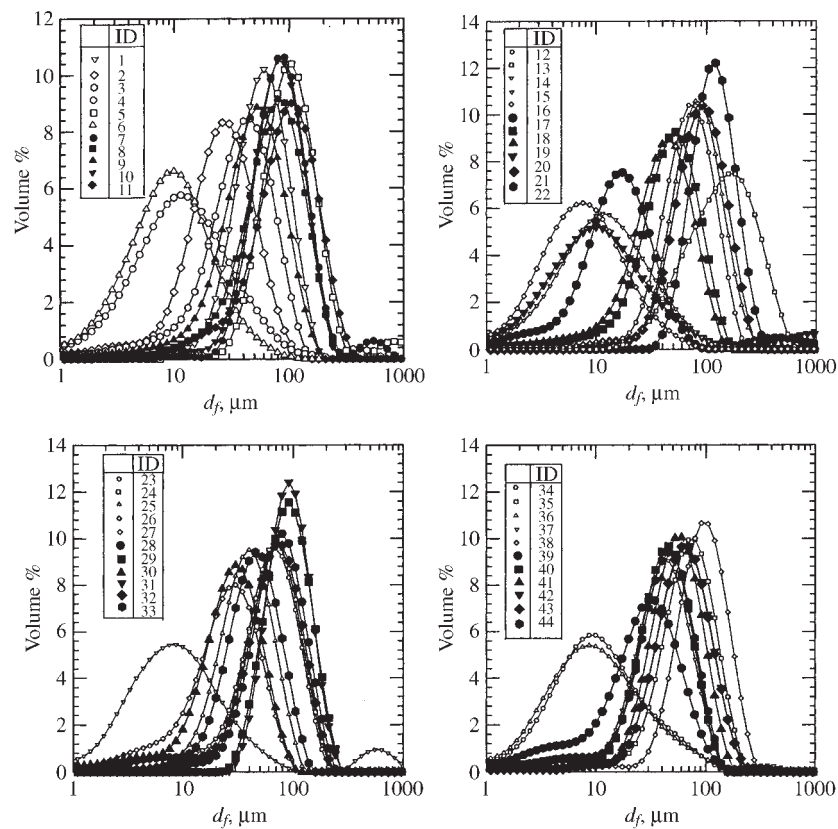


Figure 1. The floc size distributions for samples listed in Table 1.



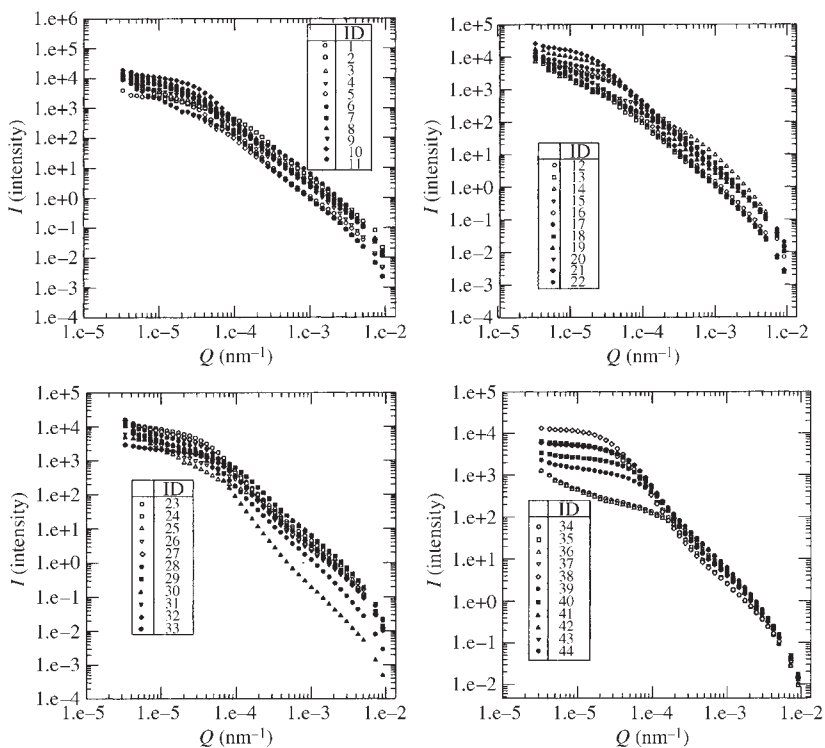


Figure 2. The log I vs. $\log Q$ plot for samples listed in Table 1.

the possibility of multiple scattering effects,^[20] whose role should be minimal for aggregates with $D_S < 2$.^[21] In the regime $-3 < \log Q < -2$, a linear $\log I$ against $\log Q$ regime yields an estimate of the mass fractal dimension of the aggregates.

Table 2 presents the average floc sizes and fractal dimensions under the experimental conditions presented in Table 1. The size of sludge flocs is large at pH 7, 14 ppm of humic acid, 80 ppm PACl , and 100 ppm NaHCO_3 , with low clay content. Meanwhile, the floc size reaches a minimum of 12.5 μm at a raw water turbidity of 200 NTU, with all other variables unchanged (6). This significant difference between floc sizes indicates the importance of mineral particles in water. Under alkaline conditions in the presence of humic acid, the generated flocs are usually larger and more compact than those obtained under acidic condition.

Figures 3 and 4, respectively, plot the supernatant turbidity and humic acid data vs. floc size and fractal dimensions. The latter two data sets are taken



Table 2. Experimental and theoretically predicted values for floc size and fractal dimensions.

ID number	$d_f (Y_1, \mu\text{m})$		Fractal dimension ($Y_2, -$)	
	Experiment	Predicted	Experiment	Predicted
1	55.7	55.5	2.19	2.19
2	30.8	32.0	1.97	1.97
3	58.2	57.9	1.81	1.81
4	40.8	42.0	2.19	2.19
5	124	125	2.00	2.00
6	12.5	13.8	2.06	2.06
7	90.1	89.8	2.13	2.13
8	70.4	70.2	1.75	1.75
9	41.2	40.7	1.93	1.93
10	77.7	77.2	1.85	1.85
11	87.1	86.5	1.91	1.91
12	63.1	62.6	1.83	1.83
13	118	118	2.11	2.11
14	66.7	68.0	2.30	2.30
15	22.4	22.1	2.06	2.06
16	31.7	32.9	2.03	2.03
17	60.1	61.5	1.82	1.82
18	27.4	27.2	2.00	2.00
19	30.7	32.2	2.07	2.07
20	87.8	87.5	1.71	1.71
21	120	120	2.08	2.08
22	125	125	2.01	2.01
23	53.4	53.0	1.93	1.93
24	60.8	60.4	1.84	1.84
25	52.7	51.2	1.92	1.92
26	8.48	2.57	2.28	2.28
27	29.9	32.8	2.11	2.11
28	43.6	42.1	1.92	1.92
29	116	115	2.03	2.03
30	30.0	29.5	1.93	1.93
31	111	110	2.07	2.07
32	65.8	65.3	1.85	1.85
33	32.5	32.3	2.05	2.05
34	26.2	27.4	2.05	2.05
35	62.9	62.7	1.95	1.95
36	27.0	28.2	2.11	2.11
37	41.0	42.2	2.00	2.00

(continued)



Table 2. Continued.

ID number	$d_f (Y_1, \mu\text{m})$		Fractal dimension ($Y_2, -$)	
	Experiment	Predicted	Experiment	Predicted
38	68.6	69.8	1.89	1.89
39	74.4	74.1	1.88	1.88
40	59.3	59.0	1.83	1.83
41	64.1	64.1	1.86	1.86
42	64.1	64.1	1.86	1.86
43	64.1	64.1	1.86	1.86
44	64.1	64.1	1.86	1.86
45	64.1	64.1	1.86	1.86
46	64.1	64.1	1.86	1.86

from the authors' earlier study.^[22] Larger flocs with a looser interior structure more efficiently remove the turbidity and humic acid.

Regression Model

The regression equation was obtained to determine the optimal values of the independent variables. Table 3 lists the fitting coefficients in the regression model, [Eq. (4)] based on the experimental data, including five linear, five quadratic, and ten interaction terms and one block term. The best-fitted, second-order polynomials are nondimensionlized using the reference variables as follows, to directly compare the significance of variables in Eq. (4); $X_{10} = 7$, $X_{20} = 14 \text{ ppm}$, $X_{30} = 100 \text{ NTU}$, $X_{40} = 100 \text{ ppm}$, and $X_{50} = 100 \text{ ppm}$. The non-dimensional equations for floc size and fractal dimension of sludge flocs are as follows.

$$\begin{aligned}
 \left(\frac{Y_1}{64.1 \mu\text{m}} \right) = & 1 - 1.07 \left(\frac{X_1}{X_{10}} \right) + 0.48 \left(\frac{X_2}{X_{20}} \right) - 0.127 \left(\frac{X_3}{X_{30}} \right) \\
 & + 8.23 \left(\frac{X_4}{X_{40}} \right) + 0.012 \left(\frac{X_5}{X_{50}} \right) - 17.7 \left(\frac{X_1}{X_{10}} \right)^2 \\
 & + 9.25 \left(\frac{X_2}{X_{20}} \right)^2 + 0.0188 \left(\frac{X_3}{X_{30}} \right)^2 - 1370 \left(\frac{X_4}{X_{40}} \right)^2 \\
 & - 0.00051 \left(\frac{X_5}{X_{50}} \right)^2 + 2.06 \left(\frac{X_1}{X_{10}} \right) \left(\frac{X_2}{X_{20}} \right)
 \end{aligned}$$



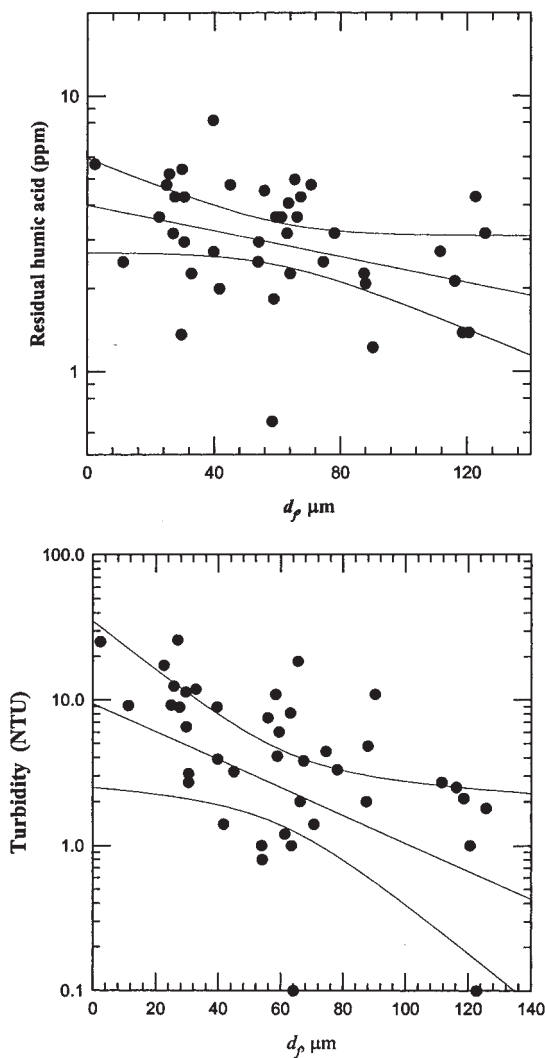


Figure 3. The supernatant turbidity and humic acid vs. floc size plot. The data of turbidity and humic acid are extracted from Annadurai et al.^[22]



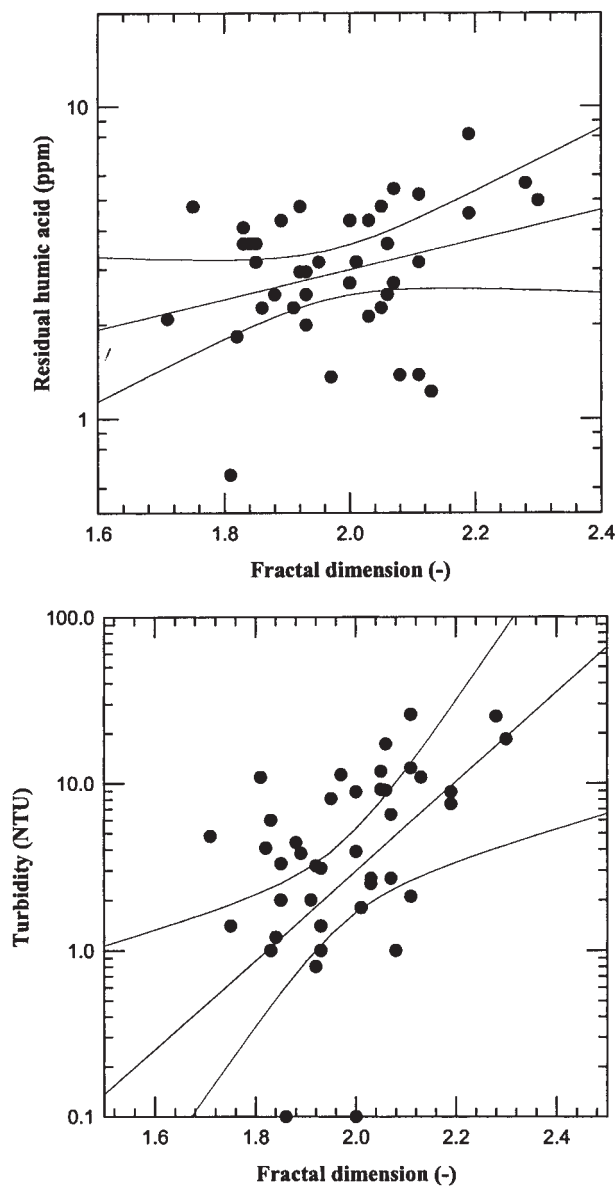


Figure 4. The supernatant turbidity and humic acid vs. floc fractal dimension plot. The data of turbidity and humic acid are extracted from Annadurai et al.^[22]



Table 3. Regression analyses for the floc size and fractal dimensions quadratic response surface model fitting (ANOVA).

Source	d_f (μm)					Fractal dimension (-)				
	Sum of squares	Degrees of freedom	Mean square	F value	p value	Sum of squares	Degrees of freedom	Mean square	F value	p value
Model	40,500	20	2020	724	<0.0001	0.81	20	0.040	12,100	<0.0001
Residual	68.8	25	2.79			8.3×10^5	25	3.3×10^6		
Lack of fit	69.8	20	3.49	6.3×10^7	<0.0001	8.3×10^5	20	4.1×10^6	6.3×10^7	<0.0001
Pure error	0.000	5	0.000			0.00	5	0.000		
Correlation	40,500	45				0.81	45			
total						R^2		R^2		
R^2	0.998	Adj R^2	0.997			0.999		Adj R^2	0.999	



$$\begin{aligned}
 & - 0.41 \left(\frac{X_1}{X_{10}} \right) \left(\frac{X_3}{X_{30}} \right) + 700 \left(\frac{X_1}{X_{10}} \right) \left(\frac{X_4}{X_{40}} \right) \\
 & - 0.080 \left(\frac{X_1}{X_{10}} \right) \left(\frac{X_5}{X_{50}} \right) + 0.022 \left(\frac{X_2}{X_{20}} \right) \left(\frac{X_3}{X_{30}} \right) \\
 & - 166 \left(\frac{X_2}{X_{20}} \right) \left(\frac{X_4}{X_{40}} \right) - 0.23 \left(\frac{X_2}{X_{20}} \right) \left(\frac{X_5}{X_{50}} \right) \\
 & + 8.94 \left(\frac{X_3}{X_{30}} \right) \left(\frac{X_4}{X_{40}} \right) + 0.0039 \left(\frac{X_3}{X_{30}} \right) \left(\frac{X_5}{X_{50}} \right) \\
 & + 3.49 \left(\frac{X_4}{X_{40}} \right) \left(\frac{X_5}{X_{50}} \right) \tag{5a}
 \end{aligned}$$

$$\begin{aligned}
 \left(\frac{Y_2}{1.86} \right) = & 1 + 0.022 \left(\frac{X_1}{X_{10}} \right) - 0.21 \left(\frac{X_2}{X_{20}} \right) - 0.010 \left(\frac{X_3}{X_{30}} \right) \\
 & - 2.36 \left(\frac{X_4}{X_{40}} \right) + 0.00059 \left(\frac{X_5}{X_{50}} \right) + 4.47 \left(\frac{X_1}{X_{10}} \right)^2 \\
 & + 0.52 \left(\frac{X_2}{X_{20}} \right)^2 + 0.0032 \left(\frac{X_3}{X_{30}} \right)^2 + 156 \left(\frac{X_4}{X_{40}} \right)^2 \\
 & + 0.000059 \left(\frac{X_5}{X_{50}} \right)^2 + 56.0 \left(\frac{X_1}{X_{10}} \right) \left(\frac{X_2}{X_{20}} \right) \\
 & - 0.051 \left(\frac{X_1}{X_{10}} \right) \left(\frac{X_3}{X_{30}} \right) - 52.6 \left(\frac{X_1}{X_{10}} \right) \left(\frac{X_4}{X_{40}} \right) \\
 & + 0.015 \left(\frac{X_1}{X_{10}} \right) \left(\frac{X_5}{X_{50}} \right) - 0.0067 \left(\frac{X_2}{X_{20}} \right) \left(\frac{X_3}{X_{30}} \right) \\
 & + 8.068 \left(\frac{X_2}{X_{20}} \right) \left(\frac{X_4}{X_{40}} \right) - 1.47 \left(\frac{X_3}{X_{30}} \right) \left(\frac{X_4}{X_{40}} \right) \\
 & - 0.0004 \left(\frac{X_3}{X_{30}} \right) \left(\frac{X_5}{X_{50}} \right) - 0.69 \left(\frac{X_4}{X_{40}} \right) \left(\frac{X_5}{X_{50}} \right) \tag{5b}
 \end{aligned}$$

Table 2 compares the experimental data with the predicted values determined from the fitted model equations. The agreement is satisfactory. The range applicable to data interpolation limits the validity of the model output. For instance, as Table 1 lists, the conditions with all the variables at low level are not included in the data analysis.

Significant Variables

Table 4 presents the results of the analysis of variance (ANOVA) for the response function (Y_i) for the coded levels of variables. The results show a



Fractal Dimensions of Flocs

33

Table 4. Coefficients of the model.

Coefficient	Value	d_f (μm)		t for H_0 : coefficient = 0	Probability $> t /$ value	Value	Standard error	Fractal dimension (-)	
		Standard error	t for H_0 : coefficient = 0					t for H_0 : coefficient = 0	Probability $> t /$ value
b_0	64.10	0.68	—	—	1.86	0.00074	—	—	$<0.0001^a$
b_1	-9.84	0.42	-23.56	$<0.0001^a$	0.041	0.00045	89.0	$<0.0001^a$	$<0.0001^a$
b_2	3.13	0.42	7.49	$<0.0001^a$	-0.040	0.00045	-87.64	$<0.0001^a$	$<0.0001^a$
b_3	-32.76	0.42	-78.40	$<0.0001^a$	-0.080	0.00045	-175.27	$<0.0001^a$	$<0.0001^a$
b_4	5.28	0.42	12.63	$<0.0001^a$	-0.044	0.00045	-97.22	$<0.0001^a$	$<0.0001^a$
b_5	7.80	0.42	18.67	$<0.0001^a$	0.02	0.00045	-21.91	$<0.0001^a$	$<0.0001^a$
b_{11}	-23.10	0.57	-40.98	$<0.0001^a$	0.17	0.00061	273.39	$<0.0001^a$	$<0.0001^a$
b_{22}	5.93	0.57	10.49	$<0.0001^a$	0.0097	0.00061	15.84	$<0.0001^a$	$<0.0001^a$
b_{33}	19.37	0.57	34.24	$<0.0001^a$	0.096	0.00061	156.08	$<0.0001^a$	$<0.0001^a$
b_{44}	-8.75	0.57	-15.46	$<0.0001^a$	0.029	0.00061	46.86	$<0.0001^a$	$<0.0001^a$
b_{55}	-3.30	0.57	-5.83	$<0.0001^a$	0.011	0.00061	18.54	$<0.0001^a$	$<0.0001^a$
b_{12}	1.89	0.84	2.26	0.0327	0.15	0.00091	164.32	$<0.0001^a$	$<0.0001^a$
b_{13}	15.23	0.84	18.23	$<0.0001^a$	-0.055	0.00091	-60.25	$<0.0001^a$	$<0.0001^a$
b_{14}	14.48	0.84	17.33	$<0.0001^a$	-0.14	0.00091	-150.62	$<0.0001^a$	$<0.0001^a$
b_{15}	-7.40	0.84	-8.86	$<0.0001^a$	-0.040	0.00091	43.82	$<0.0001^a$	$<0.0001^a$
b_{23}	0.57	0.84	0.69	0.4996	0.005	0.00091	-5.48	$<0.0001^a$	$<0.0001^a$
b_{24}	-10.69	0.84	-12.79	$<0.0001^a$	0.15	0.00091	16.43	0.0016 ^a	0.0016 ^a
b_{25}	-15.11	0.84	-18.08	$<0.0001^a$	0.00	0.00091	0.000	1.000	1.000
b_{34}	22.94	0.84	27.45	$<0.0001^a$	-0.11	0.00091	-120.50	$<0.0001^a$	$<0.0001^a$
b_{35}	10.10	0.84	12.09	$<0.0001^a$	-0.030	0.00091	-32.86	$<0.0001^a$	$<0.0001^a$
b_{45}	22.38	0.84	26.78	$<0.0001^a$	-0.13	0.00091	-147.89	$<0.0001^a$	$<0.0001^a$

^aSignificant factor.

curvilinear interactive relationship between the response function and the variables, as reflected by large mean sum of squares and the *F*-values of the total quadratic and interactive effects. The model fits the residual turbidity of the supernatant with $R^2 = 0.998$ and an *F* value of 724 at a significance level of 0.0001. Meanwhile, at the same significance level, the humic acid data fit with $R^2 = 0.999$ and *F* = 11,200.

Equations (5a) and (5b) can be used to compare the “sensitivity” of the floc size and fractal dimension to the investigated variables. The significance of the effect of the variables on the floc size follows the order, X_4 (PACl dose) $> X_1$ (pH) $> X_2$ (humic acid) $> X_3$ (raw water turbidity) $> X_5$ (alkalinity); the interactions between X_4 and X_1 or X_2 are the strongest. The significance of effect of the variables on the fractal dimension follows the order $X_4 > X_2 > X_1, X_3 > X_5$; the most influential interaction pairs are the (X_1-X_4) and (X_1-X_2) pairs. The PACl dose is the variable that most strongly affects the floc size and compactness. The effect of pH value and humic acid concentration on floc size or fractal dimension is opposite. Over the investigated range, the alkalinity of the raw water does not significantly affect the characteristics of the flocs.

Optimizing the Process

Figures 5 through 7 plot the contours of the residual turbidity and humic acid data as functions of process variables X_1-X_5 . Figure 5(a) shows that a high PACl dose preferentially produces large flocs, while turbidity significantly reduces their size. The PACl to turbidity ratio should, therefore, be high to yield large flocs. However, Fig. 5(b) shows that the high raw water turbidity is essential in yielding a loosely structured floc. For example, at a dose of 100 ppm PACl, the fractal dimension falls from 2.04 to about 1.88 as the raw water turbidity increases from 0 to 200 ppm.

Figure 6(a) and (b) shows the effects of pH and the concentration of humic acid on the characteristics of the flocs. At pH 6.5 to 7, the flocs are largest. The concentration of humic acid does not apparently affect the floc size. An acidic solution favors the production of loose flocs. The presence of humic acid promotes a reduction in the compactness of the interior of the floc. These observations indicate that the optimal pH ranges for removing turbidity and humic acid from high turbidity water are 6.5–7.5 and 5–6, respectively.^[5]

Figure 7(a) indicates that the alkalinity of the suspension only mildly affects the size and compactness of the flocs. This result correlates with the authors' earlier finding that alkalinity does not significantly affect the removal of turbidity or humic acid from water.



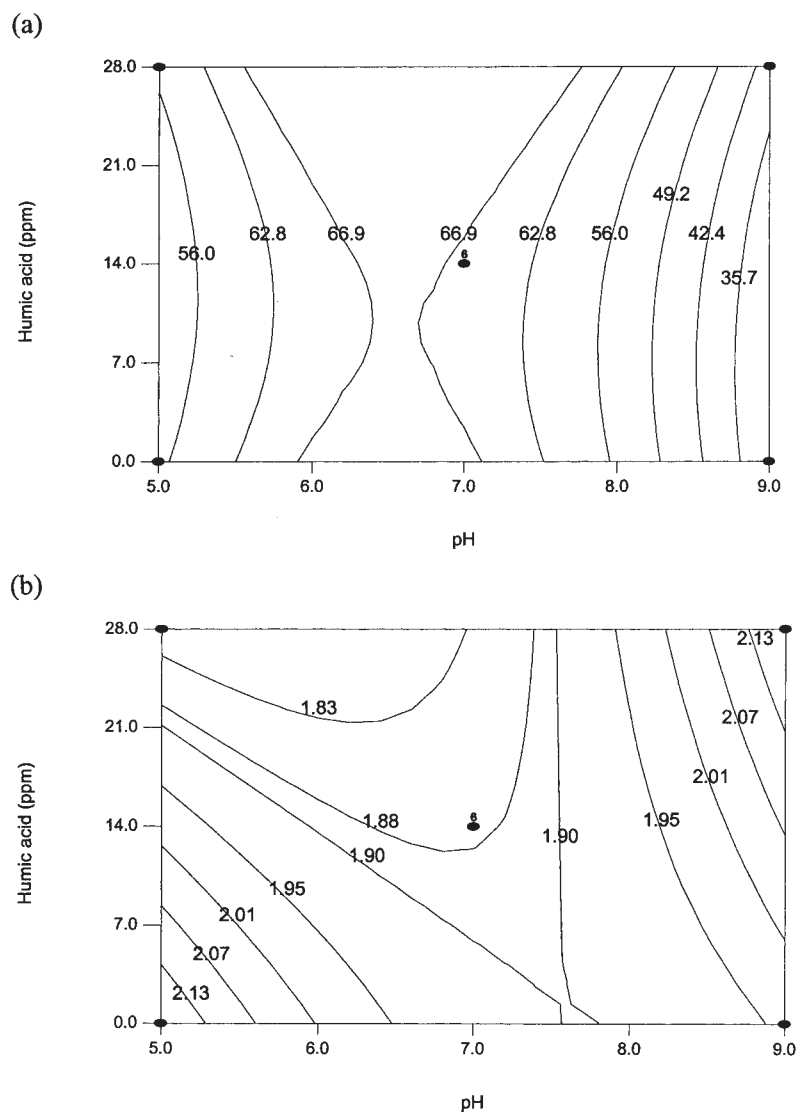


Figure 5. (a) Contour plot for d_f (μm) vs. dosed humic acid and pH value; 100 ppm PACl dose, 100 ppm NaHCO_3 , 100 NTU raw water. (b) Contour plot for fractal dimensions humic acid and pH value; 100 ppm PACl dose, 100 ppm NaHCO_3 , 100 NTU raw water.



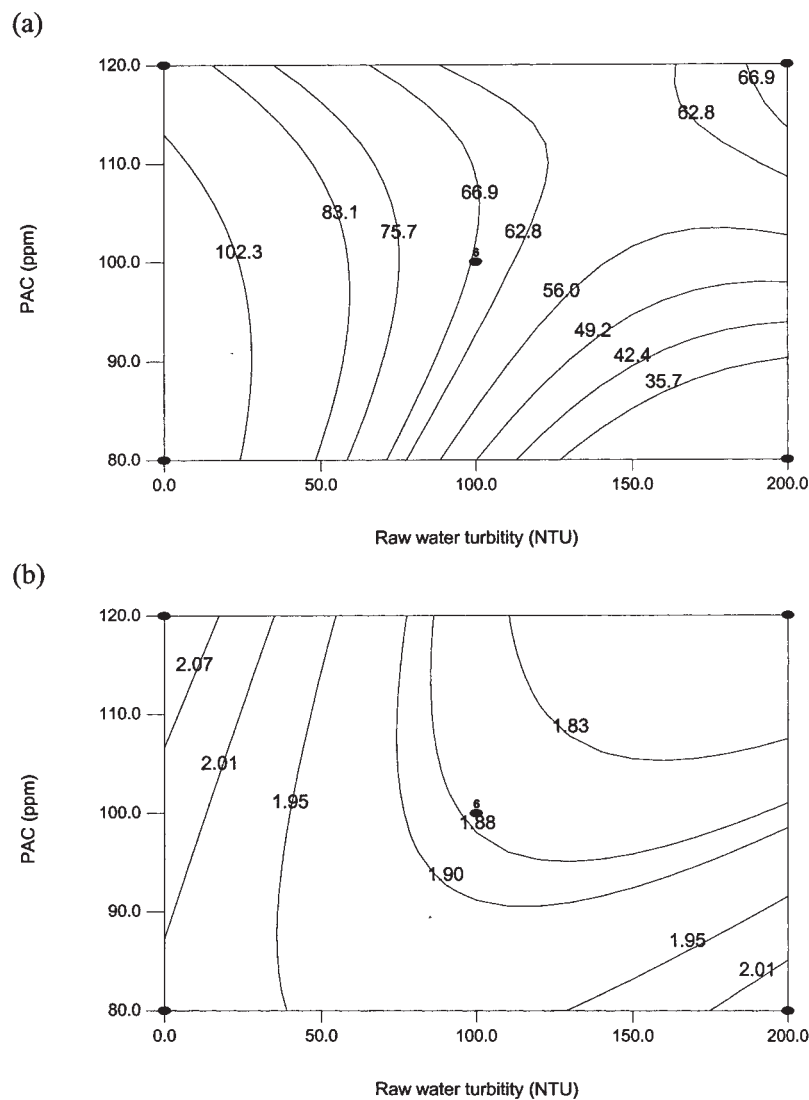


Figure 6. (a) Contour plot for d_f (μm) vs. PACl dosage and raw water; pH 7, 14 ppm humic acid dose, 100 ppm NaHCO_3 . (b) Contour plot for fractal dimensions data vs. PACl dose and raw water turbidity; pH 7, 14 ppm humic acid dosage, 100 ppm NaHCO_3 .



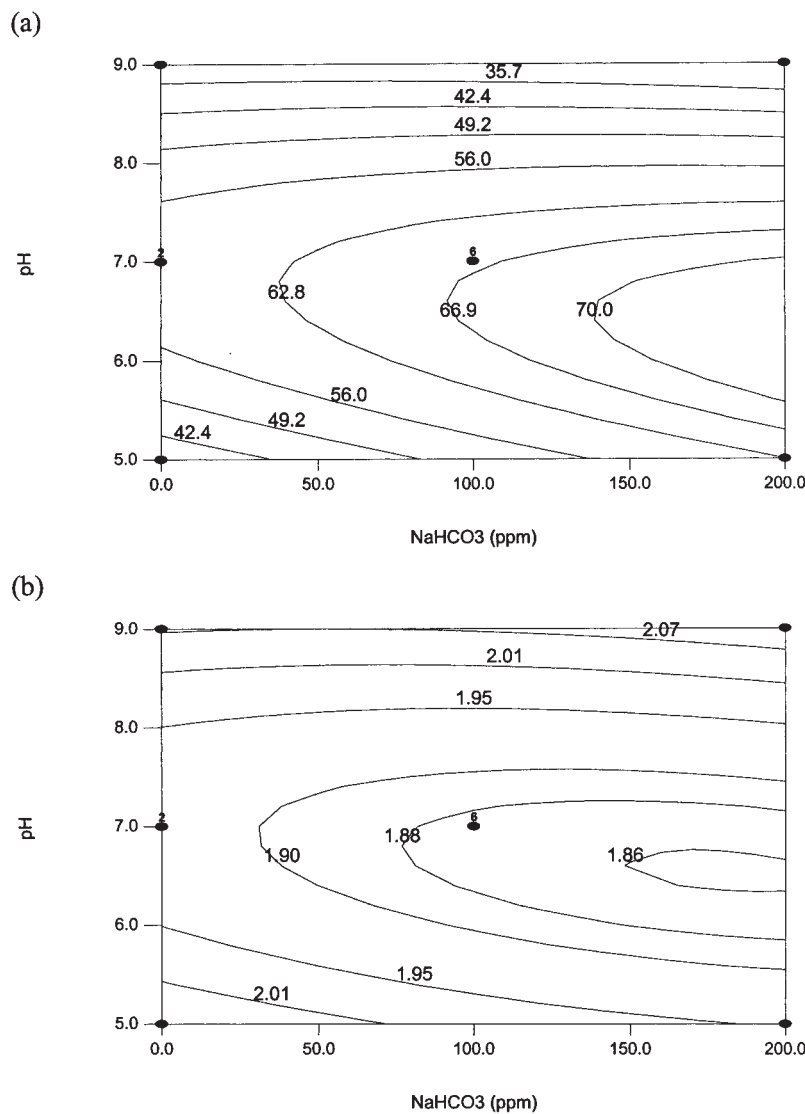


Figure 7. (a) Contour plot for d_f (μm) vs. pH value and NaHCO_3 concentration; 14 ppm dosed humic acid, 100 NTU raw water turbidity, 100 ppm PACl dose. (b) Contour plot for fractal dimensions data vs. pH value and NaHCO_3 concentration; 14 ppm dosed humic acid, 100 NTU, 100 ppm PACl dose.



The Box-Behnken design was used combined with the response surface methodology (RSM) to estimate the maximum floc size and the minimum floc fractal dimension. At pH 7, a humic acid concentration of 0–14 ppm, low turbidity, a PACl dose of 80 to 100 ppm, and over a wide range of alkalinity, the floc size can reach a maximum of 115–125 μm . Large flocs remove most of the turbidity of the suspension (see Fig. 3). Meanwhile, the fractal dimension of the flocs is a minimum at pH 5–7, a humic acid concentration of 14–28 ppm, and a raw water turbidity of 100–200 NTU over a wide range of PACl doses and alkalinites. Loose floc interiors promote the removal of humic acid (see Fig. 4). Apparently, the concentration of humic acid and the turbidity of raw water oppositely affect the size and packing characteristics of flocs. Usually, the turbidity and organic content of the raw water are not adjustable. Only the pH, PACl dose, and alkalinity of the suspension can be controlled to yield satisfactory “good” flocs for removing both turbidity and humic acid from water. As stated previously, the preferred suspension is neutral, the PACl dose is medium, and the alkalinity can be over a wide range.

Field Data

On September 16–19, 2001, tropical storm Nari hit Taiwan and brought heavy rain and serious flooding. The turbidity of the Da-Han River, which is the main surface water source for Taoyuan County, increased to 1650 NTU and the humic acid concentration increased to 1.34 ppm. The validity of these findings was tested by laboratory testing a field sample.

The pH value of the stormwater sample was first adjusted to neutral. Then, three doses of PACl were added (80, 130, and 180 ppm). The floc size distribution and the light scattering data were monitored and are plotted in Fig. 8(a) and (b). The average floc size and fractal dimension data were extracted from these curves and are presented in Table 5. In the field, most turbidity was removed at a PACl dose of 130 ppm (b). Meanwhile, the residual organic content was high in the supernatant. A 180 ppm dose (c) most effectively removed the humic acid from water. This dose, however, yielded a turbid supernatant. Tests at pH 5 and 9 were performed for comparison, and the results are also summarized in Table 5. The quality of the supernatants from these two samples was poorer than under neutral conditions.

Both samples b and c included larger flocs than the other samples. Furthermore, the fractal dimension of the samples c was lower than that of the samples b. In fact, the fractal dimension of c was the lowest of the samples collected from the field site under various operating conditions. Large flocs are required for sufficient turbidity removal, and a loose interior promotes the removal of humic acid from water. These observations are consistent with



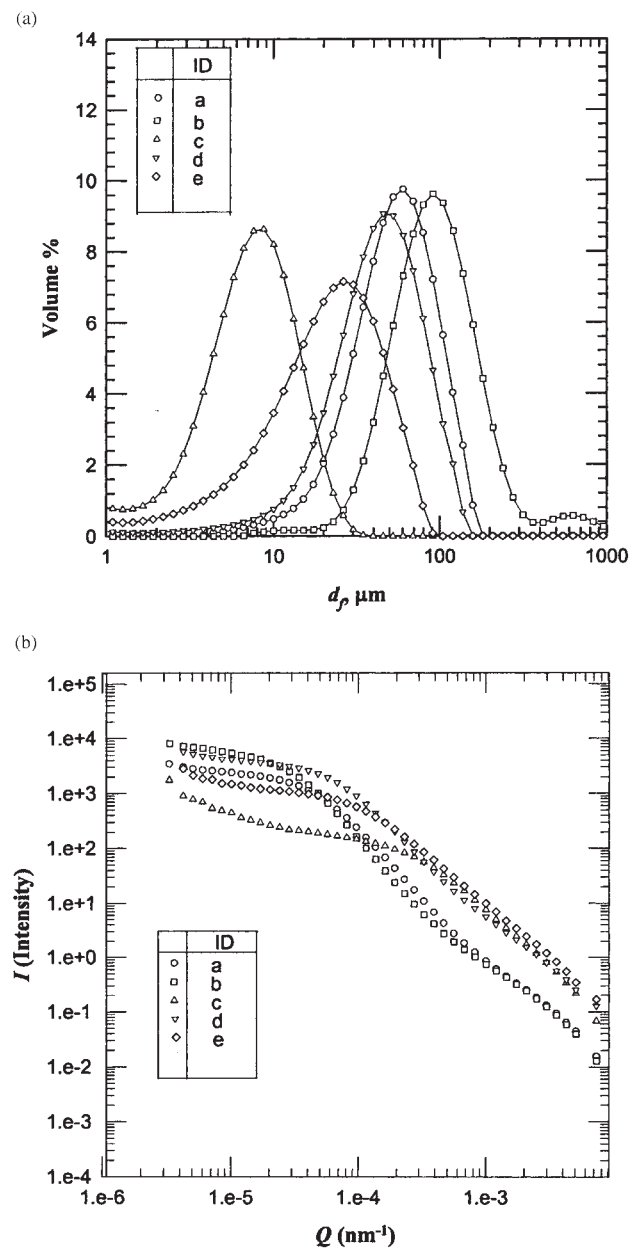


Figure 8. (a) The floc size distributions for stormwater samples listed in Table 5.
 (b) The log I vs. log Q plot for stormwater samples listed in Table 5.



Table 5. Experimental results for high turbidity raw water after the hit by tropical storm Nari.

ID number	pH	PACl dose (ppm)	d_f (μm)	Fractal dimension (–)	Turbidity (NTU)	Humic acid (ppm)
a	7	80	58.5	2.24	0.81	1.24
b	7	180	98.7	2.26	3.5	0.81
c	7	130	81.5	2.06	0.11	0.90
d	5	130	75.4	2.21	5.2	0.83
e	9	130	65.2	2.03	2.5	1.02

Note: Raw water turbidity of 1650 NTU, humic acid of 1.34 ppm.

the experimental results obtained in the bench tests. Hence, the experimental findings on the laboratory scale, for the 200 NTU samples reveal the coagulation behavior in real stormwater at very high turbidities of about 1650 NTU.

CONCLUSION

The response surface method, with the Box–Behnken experimental design, was used to examine the effects of pH, turbidity, alkalinity of suspension, the doses of polyaluminum chloride (PACl), and the humic acid on the size and fractal dimensions of flocs coagulated from highly turbid waters. Nondimensional correlations between the floc size and the fractal dimension of coagulated flocs were obtained by regression analysis. Large flocs with loose interiors favor the removal of turbidity and humic acid from water. The variable that most strongly affects the characteristics of flocs is the PACl dosage.

The “optimal” conditions for producing large flocs and for producing loose interiors are different. At pH 7, a humic acid concentration of 0 to 14 ppm, low turbidity, and a PACl dose of 80–100 ppm, over a wide range of alkalinites, the floc size can reach a maximum of 115–125 μm . Meanwhile, the fractal dimension of the flocs is minimum at pH 5–7, a humic acid concentration of 14–28 ppm, and a raw water turbidity of 100–200 NTU over a wide range of PACl doses and alkalinites. A compromise is required to yield good quality flocs for removing both turbidity and humic acid from water. The results obtained were applied to correlate the sludge floc characteristics with the treatability of the extremely high turbidity stormwater induced by storm Nari on September 16–19, 2001.



REFERENCES

1. Kawamura, S. *Integrated Design of Water Treatment Facilities*; John Wiley & Sons: NY, 1991.
2. Masschelein, W.J. *Unit Processes in Drinking Water Treatment*; Marcel Dekker: NY, 1992.
3. Rebhun, M.; Lurie, M. Control of organic mater by coagulation and flocs separation. *Water Sci. Technol.* **1993**, 27 (11), 1–20.
4. Narkis, N.; Rebhun, M. Flocculation of fulvic acids—clay minerals suspensions. Proc. 21 Annual Meeting of the Fine Particle Society, 1990; 1–25.
5. Hall, E.S.; Packham, R.F. Coagulation of organic color with hydrolysing coagulant. *J. AWWA* **1965**, 57, 1149–1166.
6. Edwards, G.A.; Amirtharajah, A. Removing color caused by humic acids. *J. AWWA* **1985**, 77, 50–57.
7. O'Melia, C.R. Practice, theory, and solid–liquid separation. *J. Water SRT—Aqua* **1991**, 40, 371–379.
8. Dempsey, B.A.; Ganho, R.M.; O'Melia, C.R. The coagulation of humic substances by means of aluminum salts. *J. AWWA* **1984**, 76, 141–150.
9. Dempsey, B.A. Reactions between fulvic acids and aluminium. In *Aquatic Humic Substances: Influence on Fate and Treatment of Pollutants*; Suffer, I.N., MacCarthy, P., Eds.; American Chemistry Society: Washington, 1989; 409–424.
10. Dentel, S.K. Application of the precipitation charge neutralization model of coagulation. *Envir. Sci. Technol.* **1988**, 22, 825–833.
11. Hundt, T.R.; O'Melia, C.R. Aluminum-fulvic acid interactions: Mechanisms and applications. *J. AWWA* **1988**, 80, 176–186.
12. Li, G.; Gregory, J. Flocculation and sedimentation of high-turbidity waters. *Water Res.* **1991**, 25, 1137–1143.
13. Cotton, A.P.; Elis, K.V.; Khowaja, M.A. Some options for water treatment in disaster situations. *J. Water SRT-Aqua* **1994**, 43, 303–310.
14. Heinzmann, B. Coagulation and flocculation of stormwaer from a separate seer system—a new possibility for enhanced treatment. *Water Sci. Technol.* **1994**, 29 (12), 267–278.
15. Zhu, H.; Smith, D.W.; Zhou, H.; Stanley, S.J. Improving removal of turbidity causing materials by using polymers as filter aid. *Water Res.* **1996**, 30, 103–114.
16. Janssens, J.G.; Buekens, A. Assessment of process selection for particle removal in surface water treatment. *J. Water SRT-Aqua* **1993**, 42, 279–288.
17. Tambo, N.; Watanabe, Y. Physical characteristics of flocs—I. The floc density function and aluminum floc. *Water Res.* **1979**, 13, 409–419.



18. Rebhun, M. Floc formation and breakup in continuous flora flocculation and in contact filtration. In *Chemical Water and Wastewater Treatment*; Hahn, H.H., Klute, R., Eds.; Springer-Verlag: Berlin, 1990; 117–126.
19. Box, G.E.P.; Behnken, D.W. Some new three levels design for the study of quantitative variables. *Technometrics* **1960**, *2*, 455–475.
20. Biggs, S.; Habgood, M.; Jameson, G.J.; Yan, Y.D. Aggregate structures formed via a bridging flocculation mechanism. *Chem. Eng. J.* **2000**, *80*, 13–22.
21. Wu, R.M.; Lee, D.J.; Waite, T.D.; Guan, J. Multi-level structure of sludge flocs. *J. Colloid Interf. Sci.* **2002**, *252*, 383–392.
22. Annadurai, G.; Sung, S.S.; Lee, D.J. Floc characteristics and removal of turbidity and humic acid from high turbidity stormwater. *J. Envir. Eng. ASCE* **2003**, *129*, 571–575.

Received August 2002

Revised July 2003



Request Permission or Order Reprints Instantly!

Interested in copying and sharing this article? In most cases, U.S. Copyright Law requires that you get permission from the article's rightsholder before using copyrighted content.

All information and materials found in this article, including but not limited to text, trademarks, patents, logos, graphics and images (the "Materials"), are the copyrighted works and other forms of intellectual property of Marcel Dekker, Inc., or its licensors. All rights not expressly granted are reserved.

Get permission to lawfully reproduce and distribute the Materials or order reprints quickly and painlessly. Simply click on the "Request Permission/Order Reprints" link below and follow the instructions. Visit the [U.S. Copyright Office](#) for information on Fair Use limitations of U.S. copyright law. Please refer to The Association of American Publishers' (AAP) website for guidelines on [Fair Use in the Classroom](#).

The Materials are for your personal use only and cannot be reformatted, reposted, resold or distributed by electronic means or otherwise without permission from Marcel Dekker, Inc. Marcel Dekker, Inc. grants you the limited right to display the Materials only on your personal computer or personal wireless device, and to copy and download single copies of such Materials provided that any copyright, trademark or other notice appearing on such Materials is also retained by, displayed, copied or downloaded as part of the Materials and is not removed or obscured, and provided you do not edit, modify, alter or enhance the Materials. Please refer to our [Website User Agreement](#) for more details.

Request Permission/Order Reprints

Reprints of this article can also be ordered at

<http://www.dekker.com/servlet/product/DOI/101081SS120027399>